DYNAMIC BEHAVIOR OF ICED OVERHEAD CABLES SUBJECTED TO MECHANICAL SHOCKS

Tamás Kálmán, Masoud Farzaneh and László E. Kollár
CIGELE / INGIVRE, Université du Québec à Chicoutimi, Québec, Canada
tkalman@uqac.ca, mfarzaneh@uqac.ca, lkollar@uqac.ca

Ghyslaine McClure
Civil Engineering and Applied Mechanics, McGill University, Québec, Canada
ghyslaine.mcclure@mcgill.ca

André Leblond
Hydro–Québec, TransÉnergie, Québec, Canada
leblond.andre.2@hydro.qc.ca

Abstract

A numerical model using nonlinear finite element analysis is proposed to calculate the dynamic effects of ice shedding induced by a pulse-type excitation on a single-span overhead line section. The excitation simulates the effect of an external load intended to remove the accreted ice from the cable; it can also simulate an accidental load due to impact or component breakage. Several ice-shedding scenarios are studied with variables including ice thickness, line parameters such as span length, cable tension, and pulse-load characteristics. This model serves as a basis to study various failure criteria of atmospheric glaze ice in terms of stress-strain relations and strain-rate effects. The failure criteria defined for glaze ice incorporate both axial and bending effects.

INTRODUCTION

The main loads applied to transmission line structures come from the cables they support. In cold regions prone to atmospheric icing, overhead transmission lines are among the most vulnerable structures as they may collect ice from storms of large footprint. It is well known that ice deposits on cables can be the source of several mechanical problems.

Numerical modeling of ice shedding on overhead transmission lines

The dynamic analysis of transmission lines subjected to shock loads is complex. Such shock loads may result from the effect of an external load intended to remove accreted ice from the cable. More generally, they can also be caused by accidental loads due to impact or component breakage. In most previous studies of ice shedding from lines [1-3], the line response to instantaneous shedding was modeled, whereas in this research, the failure propagation of the ice deposit along the span is studied. Combining the two approaches would provide a powerful simulation tool for several practical industrial applications for ice accretion mitigation on overhead lines.

Small-scale experiments and finite element modeling were performed to study the effect of ice shedding on overhead lines by Jamaleddine et al. [1]. In this study, ice shedding was simulated experimentally by the sudden drop of dead weights, and a nonlinear dynamic finite element model was developed using ADINA [14]. Comparison of the experimental and numerical results confirmed the modeling capabilities of both static and dynamic analyses.

Following Jamaleddine's work, a numerical study of a two-span line section response to instantaneous shedding was undertaken by Roshan Fekr and McClure [2]. A total of 21 ice-shedding scenarios were studied with variables including: ice thickness, span length, difference in elevation

between end and suspension points, number of spans per line section, presence of unequal spans and partial ice shedding on sub-spans. The numerical simulations were also carried out using ADINA.

Mechanical properties of glaze ice

Atmospheric icing may take place at temperatures between -10 and 0°C or, sometimes, at lower temperatures under particular conditions. The occurrence, severity, and type of atmospheric icing depend very much on temperature, wind speed, total water content of the air, and water droplet dimensions. The types of atmospheric ice accreted on transmission lines that are of important mechanical concern are heavy adherent wet snow, large but lightweight rime ice, and dense glaze ice [6, 11].

Ice is a very complex material. Its mechanical properties depend among other things on crystal structure, temperature, presence of impurities, and type and rate of loading. In short-term loading, ice behaves elastically and fails in a brittle manner. If the loading rate is low (below 10^{-3} s^{-1}), creep and plastic failure predominate [6]. In this study, the properties of ice associated with short-term loading are assumed to prevail.

In the case of mechanically-induced ice breaking by shock loads, the main properties that govern the failure of accreted ice on cables relate to the tensional (axial) and flexural rigidities of the iced section. On the basis of observations and numerical simulations, the authors suggest that the flexural properties of the ice deposit are mainly responsible for the mechanical ice-shedding phenomenon. However, information about the mechanical properties of dense glaze ice under high strain rate (above 10^{-3} s^{-1}) is lacking.

Ice in tension behaves in a brittle manner at much lower strain rate than in compression [6-9]. Investigations of the brittle failure of polycrystalline fresh-water ice by Schulson [7] indicate that ice generally exhibits negligible tensile ductility. The tensile strength of fresh water ice appears to decrease with increasing grain size and to be independent of strain rate, and only slightly dependent on temperature. Under compression, fresh water ice exhibits brittle behavior only at high strain rates: the strength decreases with increasing temperature, strain rate and grain size. Characterization of the flexural properties of fine-grained fresh-water ice at low deformation rates [12] indicates that the flexural strength is not a function of the loading rate. However, it is believed that the flexural strength of ice at high deformation rates is rate-dependent.

Despite much research effort in the last few decades, information about the mechanical properties of atmospheric ice in natural conditions is still lacking. However, both the analysis of ice samples collected by Laforte et al. [10] from transmission lines after significant ice storms, and the experiments of Druez et al. [9] on the ductile-brittle transition of laboratory glaze ice under compression, indicate that the mechanical properties of fine-grained fresh-water ice are a reasonable assumption for this study.

GENERAL NUMERICAL APPROACH

As in previous numerical studies [1, 2], ADINA [14] is used here to simulate the dynamic effects of ice shedding induced by a pulse-type excitation on a level single-span line section. A total of 27 ice-shedding scenarios are studied with variables including ice thickness, line parameters such as span length, cable tension and pulse-load characteristics. The flexibility of the towers and their foundations is not modeled and the cable ends are assumed rigidly fixed.

Cable modeling

The cable is assumed to be perfectly flexible in bending and torsion; therefore it is modeled with 2-D two-node isoparametric truss elements using a total Lagrangian formulation with large displacement

kinematics but small strains [14, 15]. Each cable element has four degrees-of-freedom corresponding to the horizontal and vertical translations at each end. The cable material properties are patterned as if it was made of elastic material reacting to tension only therefore allowing slackening whenever the cable loses its prestressing force. For each 0.2 m long element, an initial strain value is prescribed as calculated from a preliminary static analysis for an axially rigid catenary under its self-weight. The finite element mesh selection is based on dynamic considerations discussed below.

Accreted ice modeling

Accreted ice on the cable is modeled as a separate nonlinear 2-D two-node plane stress iso-beam element in parallel to each cable element. For the plane stress element, it is assumed that the out-of-plane stress is equal to zero. Using the 2-D beam option instead of the general 3-D beam reduces the computational effort considerably for this simple single-span model [14]. Each iso-beam element has six degrees-of-freedom corresponding to the horizontal and vertical translations and the in-plane rotation. Since only rectangular cross sections can be considered for the materially nonlinear iso-beam element in ADINA, the cross-sectional parameters of the beam ice deposit are specified to yield a bending stiffness equivalent to the idealized shape of accreted ice. In order to avoid spurious stiffening of the system caused by fixed rotational boundary conditions at the supports, iso-beam elements are omitted just next to the support nodes.

Damping

Aerodynamic damping is neglected and only structural damping of the iced cable is considered. Therefore, damping is modeled by using a non-linear axial dashpot element in parallel to each cable element [14]. The selection of the damping constant is discussed in more details by Roshan Fekr et al. [2] and McClure and Lapointe [4]. In this study the damping constant is set to represent an equivalent viscous damping of 2.6% critical. Besides this viscous structural damping, algorithmic (numerical) damping is introduced to filter out spurious high frequencies of the response due to finite element discretization. Numerical damping is introduced with the Newmark-β integration operator with parameters $\delta = 0.55$ and $\alpha = 0.3$ relying on previous work [5].

Static equilibrium

In order to avoid the stiffening effect of the flexural rigidity of the ice iso-beam on the initial static profile, the deformed cable profile is calculated beforehand using an increased density cable model as in previous studies [1, 2 and 4]. This deflected static profile serves as the initial profile of the ice-cable composite model where the cable element is initially prestressed by setting the initial strain to the value obtained from static analysis of the increased density cable model.

Dynamic analysis

A Restart option is available in ADINA to start the dynamic analysis from the initial static equilibrium profile obtained for the iced cable. Static analysis is completed in 5 load increments so that dynamic analysis is started at time $t = 5$. The pulse-type excitation is defined as a concentrated vertical upward force applied at the mid span joint. It is a triangular pulse (the magnitude is varied) of 3 ms duration. The load is activated at time $t = 5$ for 10 time steps of 0.3 ms. The selection of the time step and the mesh size is such as to provide adequate sampling of the shock wave as it travels through the cable finite element mesh [5]. A lumped mass formulation is used throughout. As previously indicated, the Newmark-β direct implicit integration method is used to solve the equilibrium equations, with the full Newton-Raphson iteration method for stiffness updates [14, 15].

Ice failure modeling

Ice failure and subsequent shedding or detachment is modeled using the *"element death upon rupture"* option available in ADINA. For the ice (iso-beam) element with plastic bilinear material model, the element death option is automatically activated when the rupture criterion is fulfilled at any integration point of the element. The element is then considered as "dead" for the remainder of the analysis and its mass and stiffness contributions are removed from the model [14]. The ice material model is defined in ADINA by setting the Young's modulus to 10 GPa, the Poisson's ratio to 0.33, the initial yield stress to 2 MPa, and the maximum allowable effective plastic strain to 10^{-10}.

RESULTS

Eigenvalue analysis

Several natural frequencies and mode shape analyses were conducted on various iced span models to validate and adjust the parameters of the mesh and investigate alternate modeling approaches. In all cases, the cable was modeled with the prestressed truss elements while the ice deposit was represented by either the increased-density truss element, the Hermitian beam element or the iso-beam element, respectively. The calculated mode shapes and corresponding natural frequencies were identical in all models and comparable to those obtained from Irvine's theory [13]. These investigations proved the applicability of modeling the ice deposit with the iso-beam element hence the further applicability of the newly developed iced cable model for ice-shedding simulations.

Transient dynamic analysis

Results of one case with parameters summarized in Table 1 are presented in some details to illustrate the calculated dynamic response of iced cables subjected to mechanical shocks. The axial response in both the cable and the ice deposit, as well as the flexural response of the ice deposit, are monitored. In this case, ice is modeled as a linear isotropic material to avoid its rupture so that the dynamic response of the fully iced cable can be examined. Figure 1 displays vertical displacement and cable tension histories at various points. Figure 2 shows both axial and bending effects of the shock load on the ice deposit. Amplitude of the shock point load is set to 30 kN at this stage of analysis.

The shock point load applied to the cable at mid span generates transverse waves that propagate along the span, causing significant bending of the ice deposit at high deformation speed. The wave propagation can be seen in Figures 1a and 1b where the vertical displacement of the iced cable is shown both at the mid span excitation point and close to the support. The mid span displacement (Fig. 1a) is clearly dominated by low frequency oscillations combined with smaller amplitude higher frequency content. The latter is more pronounced for vertical displacements near the fixed support (Fig. 1b). As expected, the shock load generates additional cable tension and the frequency content of the signature is higher than for transverse displacements. Cable tensions at the excitation point do not exceed those at the support when ice detachment is not considered (Figs. 1c and 1d). However, the converse is observed in the transient phase when ice failure and shedding is modeled (Fig. 3d).

The numerically-generated high frequency content of the response is partly filtered out by the numerical integration operator. However, high frequency oscillations are still present, which correspond to the fundamental longitudinal vibration of the iced cable (evaluated at 4 Hz).

The time histories presented in Figure 2 show that both the axial and bending deformation rates calculated are high enough to assume ice mechanical properties at high strain rate. However, as expected, bending effects in the ice deposit are more significant than axial effects and should govern the failure. Bending strain rates and corresponding stresses and strains in the ice deposit (Figs. 2d, e and f) are high enough to expect ice failure in a brittle manner.

Table 1. Parameters of the case study

Line parameter		**Conductor parameter**	
Span length (m)	300	Name	CONDOR
Difference in elevation (m)	0	Type	ACSR 54/7
Initial sag-span ratio (%)	5	Overall diameter (mm)	27.762
Ice parameter		Total cross sectional area (mm^2)	455.03
Type	Glaze	Modulus of elasticity (GPa)	68.95
Density (kg/m^3)	900	Mass per unit length (kg/m)	1.5239
Radial ice thickness (mm)	25	Rated tensile strength (kN)	125.44

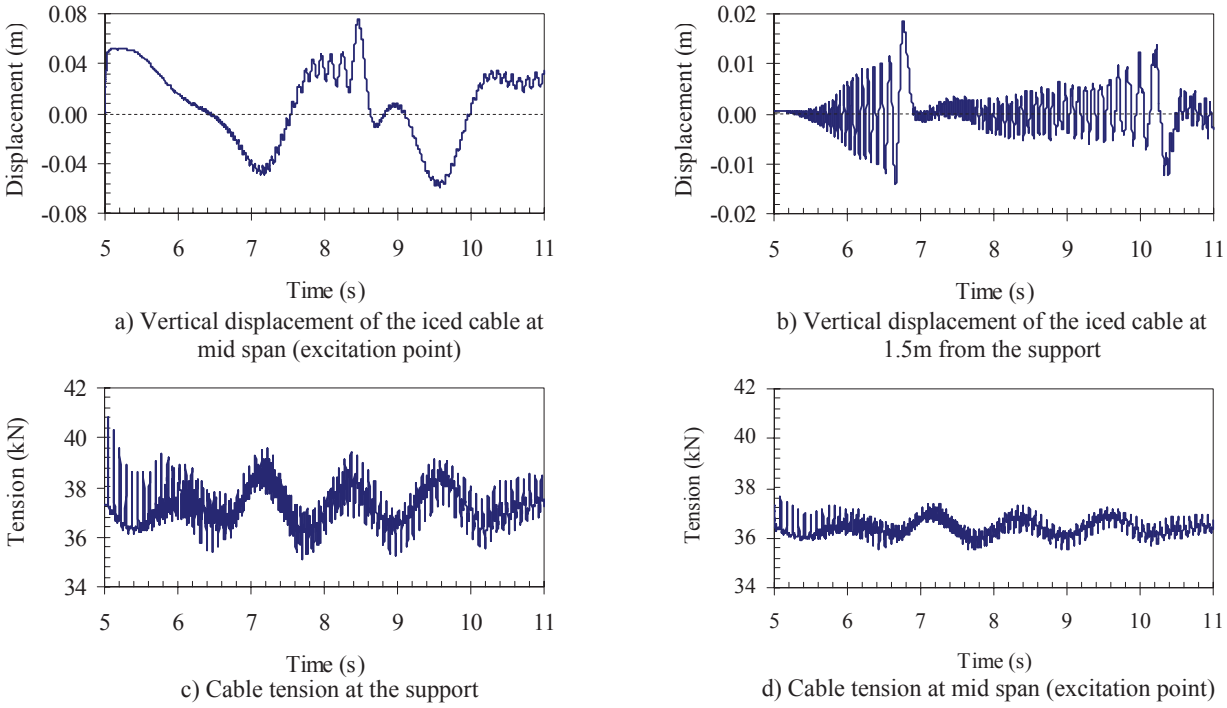

a) Vertical displacement of the iced cable at mid span (excitation point)

b) Vertical displacement of the iced cable at 1.5m from the support

c) Cable tension at the support

d) Cable tension at mid span (excitation point)

Figure 1. Dynamic response of an iced cable subjected to a shock load

Ice shedding scenarios

A total of 27 ice shedding scenarios are studied with variables including: ice thickness (10mm, 25mm and 38mm), line parameters such as span length (100m, 200m and 300m), cable tension and pulse-load characteristics. Different pulse-load characteristics are represented by the variation of load amplitude (30kN, 45kN and 60kN) while the pulse duration is kept constant at 3 ms. For all cases the static catenary profile and the iced static profile are calculated (Table 2). A summary of the results is presented in Table 3, which lists the rate of ice shedding (R.I.S.), i.e. the fraction of the ice shed in the span, the maximum cable tension at the excitation point (M.T.) and at the support (M.T.S.) as well as the maximum cable jump. Zero displacement refers to the fully iced cable configuration. Figure 3 presents selected time histories of vertical cable jumps at mid span and cable tensions, for the case where 20% of the ice sheds (Figs. 3 a, b and d) and for 100% shedding (Fig. 3c).

Model results indicate that a sudden load with amplitude of 30kN is sufficient to fully remove thin (10mm) accreted ice on a 300m span. The larger the ice thickness and span length are, the larger is the amplitude of the shock load necessary to shed the ice. However, in this numerical study, a load of 60kN generated additional tension in the cable at the excitation point that exceeded the rated tensile strength of the cable, which is unrealistic. Therefore, to avoid damaging the cable, it may be necessary to apply successive lower amplitude shock loads at a given point along the span or at two or more points. To verify this scenario, a hypothetical example was simulated for a 300m span with 38mm

radial ice thickness using two synchronous shock loads with amplitude of 45kN located at about one quarter span length from both supports. The results have confirmed that this approach may be safe and effective: the ice shedding percentage increased from 15% (with one shock load at mid span) to about 40% without reaching the load limit of the cable and/or the structure.

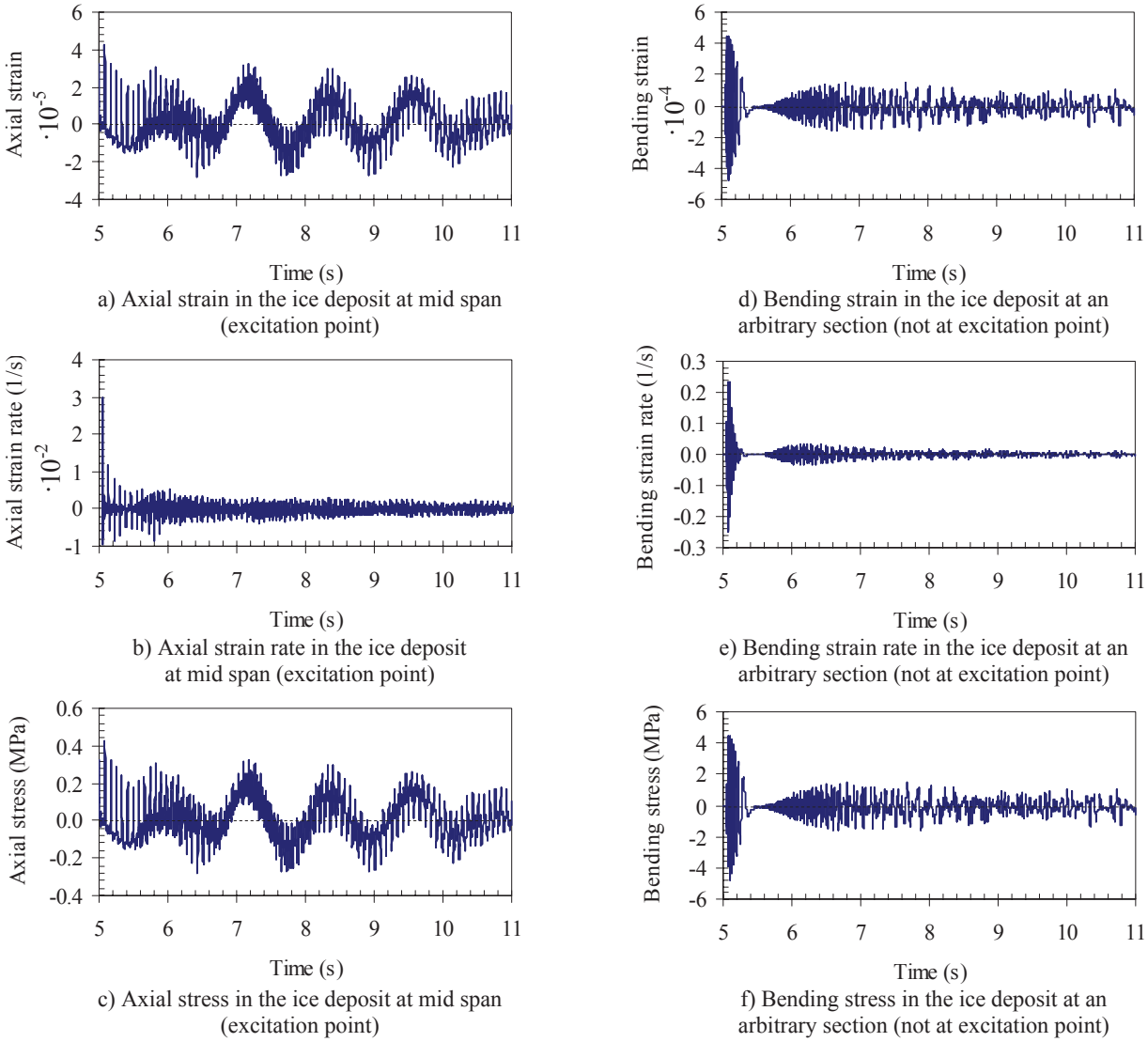

a) Axial strain in the ice deposit at mid span (excitation point)

d) Bending strain in the ice deposit at an arbitrary section (not at excitation point)

b) Axial strain rate in the ice deposit at mid span (excitation point)

e) Bending strain rate in the ice deposit at an arbitrary section (not at excitation point)

c) Axial stress in the ice deposit at mid span (excitation point)

f) Bending stress in the ice deposit at an arbitrary section (not at excitation point)

Figure 2. Axial and bending effects in the ice deposit under shock load

Table 2. Static cable tensions and sags

Span (m)	Radial ice thickness (mm)	Catenary state		Iced span	
		Tension (kN)	Max. sag (m)	Tension (kN)	Max. sag (m)
100	10	3.81	5.017	6.44	5.049
	25	3.81	5.017	12.87	5.125
	38	3.81	5.017	20.69	5.215
200	10	7.62	10.036	12.81	10.159
	25	7.62	10.036	25.27	10.449
	38	7.62	10.036	40.09	10.783
300	10	11.43	15.053	19.10	15.328
	25	11.43	15.053	37.26	15.953
	38	11.43	15.053	58.47	16.652

Table 3. Ice shedding scenarios

Span (m)	Load (kN)	Radial ice thickness											
		10 mm (1.07 kg/m)				25 mm (3.73 kg/m)				38 mm (7.07 kg/m)			
		R.I.S	M.T.	M.T.S	M.D.	R.I.S.	M.T.	M.T.S	M.D	R.I.S.	M.T.	M.T.S	M.D.
100	30	100	76.36	65.18	0.71	70	67.28	29.98	0.54	20	58.84	42.78	0.16
	45	100	105.9	99.48	0.87	100	93.30	27.78	0.68	70	92.43	42.75	0.41
	60	100	142.0	142.0	1.21	100	130.63	32.58	0.68	95	114.5	40.88	0.65
200	30	100	77.78	23.28	0.49	15	73.06	36.06	0.40	10	69.99	56.78	0.22
	45	100	107.0	64.80	0.75	50	98.77	40.72	0.68	15	97.18	57.01	0.35
	60	100	133.6	59.50	0.99	100	134.3	38.21	0.90	20	122.9	57.69	0.75
300	30	100	76.62	29.12	0.48	20	78.89	49.08	0.42	10	83.94	76.38	0.12
	45	100	102.6	45.52	0.68	25	104.8	51.96	0.87	15	107.5	72.42	0.37
	60	100	131.8	57.19	0.80	100	138.3	54.12	1.11	40	132.5	70.53	0.55

R.I.S. - Rate of ice shedding (%)
M.T. - Maximum cable tension (at excitation point) (kN)
M.T.S. - Maximum cable tension at support (kN)
M.D. - Maximum mid span displacement (m)

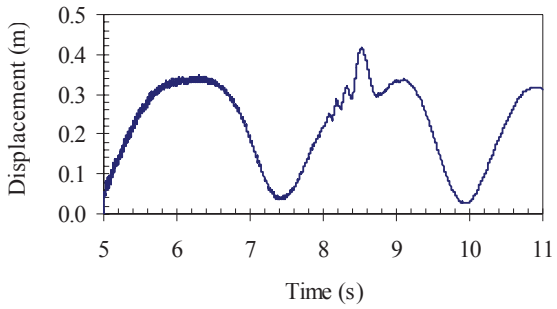

a) Vertical displacement at mid span due to shock load causing 20% ice shedding (span: 300m; ice thickness: 25mm; load: 30kN)

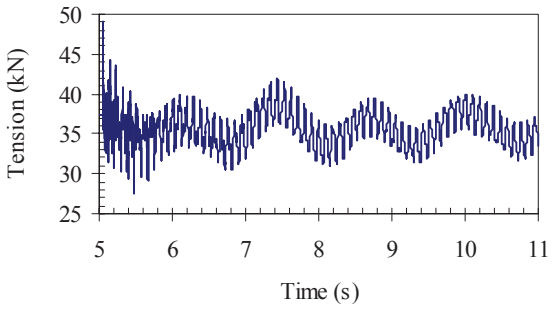

b) Cable tension at the support due to shock load causing 20% ice shedding (span: 300m; ice thickness: 25mm; load: 30kN)

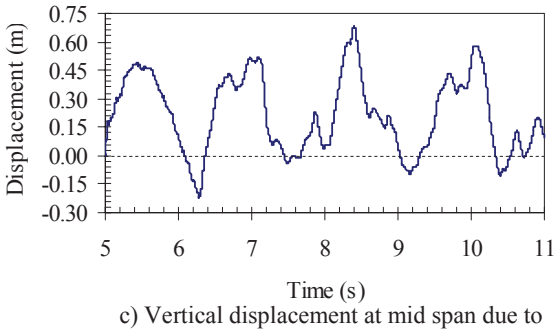

c) Vertical displacement at mid span due to shock load causing 100% ice shedding (span: 100m; ice thickness: 25mm; load: 45kN)

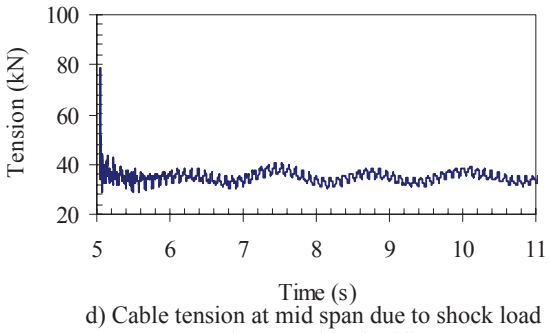

d) Cable tension at mid span due to shock load causing 20% ice shedding (span: 300m; ice thickness: 25mm; load: 30kN)

Figure 3. Transient dynamic response of cable to shock load inducing ice shedding

CONCLUSIONS

The finite element model presented can serve as a basis to study various failure criteria of atmospheric glaze ice in terms of stress-strain relations, and strain-rate effects. Further refinements of the failure criteria of atmospheric ice can be integrated to this model as they become available. Various line section geometries can also be easily investigated using the model. However, experimental validation of the model results in real scale is paramount.

This study has shown that it is feasible to model the effects of ice shedding induced by a shock load on single-span overhead transmission cables. To our knowledge, this is the first time such a numerical

model is presented where the rupture of the ice deposit is explicitly considered. We envision that similar models will provide a powerful simulation tool to assist in the management of mitigation for atmospheric icing on lines.

Acknowledgment

This research was carried out within the framework of the NSERC / Hydro-Québec Industrial Chair on Atmospheric Icing of Power Network Equipment (CIGELE) and the Canada Research Chair on Atmospheric Icing Engineering of Power Network (INGIVRE) at the University of Québec at Chicoutimi (UQAC), and the Department of Civil Engineering and Applied Mechanics at McGill University. The authors would like to thank all the sponsors of the CIGELE for their financial support.

REFERENCES

[1] A. Jamaleddine, G. McClure, J. Rousselet, and R. Beauchemin, 1993, "Simulation of ice shedding on electrical transmission lines using ADINA", *Computers and Structures,* vol. 47, No. 4/5, 523-536.

[2] M. Roshan Fekr and G. McClure, 1998, "Numerical modeling of the dynamic response of ice shedding on electrical transmission lines", *Atmospheric Research,* vol. 46, 1-11.

[3] M. Matsuura, H. Matsumoto, Y. Maeda, and Y. Oota, 1995, "The study of ice shedding phenomena on transmission lines", *Proceedings of International Symposium on Cable Dynamics*, AIM , Liege, Belgium, 19-21 October, 181-188.

[4] G. McClure and M. Lapointe, 2003, "Modeling the structural dynamic response of overhead transmission lines", *Computers and* Structures, vol. 81, 825-834.

[5] G. McClure and R. Tinawi, 1987, "Mathematical modeling of the transient response of electric transmission lines due to conductor breakage", *Computers and* Structures, vol. 26, No. 1/2, 41-56.

[6] E. Eranti and G.C. Lee, 1986, *Cold Region Structural Engineering*, McGraw-Hill Inc., NY.

[7] E.M. Schulson, 2001, "Brittle failure of ice", *Engineering Fracture Mechanics*, vol.68, 1839-1887.

[8] J.J. Petrovic, 2003, "Review: Mechanical properties of ice and snow", *Journal of Materials Science*, vol. 38, 1-6.

[9] J. Druez, D.D. Nguyen and Y. Lavoie, 1986, "Mechanical properties of atmospheric ice", *Cold Regions Science and Technology,* vol. 13, 67-74.

[10] J-L. Laforte, C.L. Phan, D.D. Nguyen, and B. Félin, 1982, "Determining atmospheric parameters during ice accretion from the microstructure of natural ice samples", *Proceedings of First International Workshop on Atmospheric Icing of Structures*, CRREL Special Report 83-17, Hanover, NH, USA, 1-3 June, 75-184.

[11] S. C. Colbeck, S. F. Ackley, 1982, "Mechanism for ice bonding in wet snow accretions on power lines", *Proceedings of First International Workshop on Atmospheric Icing of Structures*, CRREL Special Report 83-17, Hanover, NH, USA, 1-3 June, 25-30.

[12] G.W. Timco and R.M.W. Frederking, 1982, "Comparative strength of fresh water ice", *Cold Regions Science and Technology,* vol. 6, 21-27.

[13] H.M. Irvine, 1981, *Cable structures*, MIT Press, Cambridge, MA, USA.

[14] ADINA R&D Inc., 2004, *ADINA Theory and Modeling Guide*, September 2004, Watertown, MA, USA.

[15] K.J. Bathe, 1996, *Finite element procedures*, Prentice Hall, Upper Saddle River, NJ, USA.